Physics

Electricity & Magnetism fields

Okayama University *Year* 1991

3-D finite element analysis of coupling current in multifilamentary AC superconducting cable

Norio Takahashi* Takayoshi Nakata† Y. Fujii‡
Kazuhiro Muramatsu** M. Kitagawa†† Jun Takehara‡‡

*Okayama University
†Okayama University
‡Okayama University
**ALPS Electric Company Limited, Miyagi
††Chugoku Electrir Power Corporation
‡‡The Chugoku Electric Power Corporation, incorporated

3-D FINITE ELEMENT ANALYSIS OF COUPLING CURRENT IN MULTIFILAMENTARY AC SUPERCONDUCTING CABLE

N.Takahashi*, T.Nakata*, Y.Fujii*, K.Muramatsu**, M.Kitagawa*** and J.Takehara***

* Dept. of Elec. Eng., Okayama University, Okayama, Japan
** Central Lab., ALPS Electric Co., Kakuda, Japan
*** Technical Research Inst., Chugoku Electric Power Co., Oono, Hiroshima, Japan

Abstract - A new method for analyzing the 3-D coupling current which is induced by an ac magnetic field in a multifilamentary superconducting cable is developed. In this method, such a superconducting cable, in which many twisted filaments are embedded in a matrix, is treated as macroscopic, having anisotropic conductivity. The method for treating the anisotropy of conductivity and the 3-D finite element formulation are presented. The effectiveness of the technique is illustrated by the analysis of the 3-D coupling currents of superconducting cables.

1. INTRODUCTION

In order to develop an ac multifilamentary superconducting cable[1] which carries heavy current at low loss, the 3-D coupling current[2] should be reduced. As the structure of the superconducting cable is 3-dimensional and complicated, a practical 3-D numerical method should be developed. The analysis of the 3-D coupling current using the usual 3-D finite element method[3] is difficult, because a large number (e.g. 20000) of fine filaments, of which the diameter is small (e.g. 0.5μm), are embedded in a metallic matrix. Some researchers have reported only an theoretical analysis[2] and a 2-D numerical analysis[4].

In this paper, a new method for analyzing 3-D coupling current in multifilamentary superconducting cable is developed taking efficiently into account the anisotropy of conductivity of filament (superconductor) and matrix(CuNi). The calculated value of the coupling loss in a strand is compared with the theoretical value, and the 3-D complicated coupling currents in stabilized superconducting cables are analyzed.

2. METHOD OF ANALYSIS

2.1 Modelling of Multifilamentary Cable

When there are many twisted filaments in a superconducting cable, it is difficult to analyze magnetic fields in the multifilamentary cable using the conventional 3-D finite element method, because the number of finite elements increases greatly. If the multifilamentary strand in the cable is treated as a macroscopic one having anisotropic conductivity, as shown in Fig.1, the calculation can be carried out within the acceptable computer storage and CPU time.

The conductivity $\sigma_{//}$ parallel to the filament is equal to infinity. The conductivity $\sigma_{\perp}$ perpendicular to the filament can be given by[2]

$$\sigma_{\perp}=\frac{1+\lambda}{1-\lambda}\sigma_m \qquad (1)$$

where σ_m is the conductivity of the normal metal matrix, which is used to stabilize the superconductor. λ is the volume fraction of superconductor in the strand.

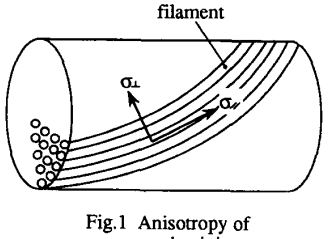

Fig.1 Anisotropy of conductivity.

(a) Strand

Let us investigate the relationship between the current density J and the electric field strength E in the strand shown in Fig.2. The z-axis is the center line of the strand. The unit vectors e_u, e_v and e_w in the u-, v- and w-directions at a point P on the filament are assumed as shown in Fig.2(a) in order to prescribe the direction of the filament. e_w is tangential to the filament. e_u and e_v are both normal to the filament. e_v is tangential to the coaxial cylinder, of which the radius is equal to O-P, and e_u is normal to the coaxial cylinder.

The relationship between e_x, e_y and e_z (unit vectors in the x-, y- and z-directions) and e_u, e_v and e_w can be obtained by the following processes: Firstly, unit vectors e_{xa}, e_{ya} and e_{za} shown in Fig.2(b) are introduced. These vectors are obtained by rotating e_x, e_y and e_z by θ_1 about the z-axis as shown in Fig.2(b). θ_1 is the angle between the e_x and e_{xa} vectors. Secondly, e_u, e_v and e_w vectors are obtained by rotating e_{ya} and e_{za} vectors by θ_2 about the e_{xa} vector. θ_2 is the angle between the e_z and e_w vectors as shown in Fig.2(a). Therefore, the relationship between Jx, Jy and Jz and Ju, Jv and Jw can be written as follows:

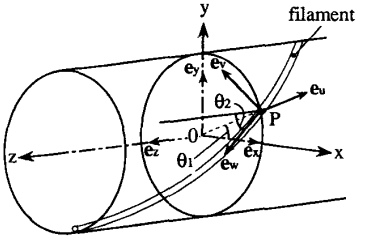

(a) unit vectors e_u,e_v,e_w

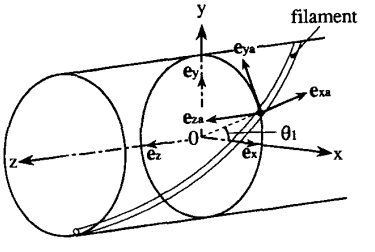

(b) unit vectors e_{xa},e_{ya},e_{za}

Fig.2 Strand.

0018-9464/91$01.00 © 1991 IEEE

$$\begin{Bmatrix} Jx \\ Jy \\ Jz \end{Bmatrix} = \begin{bmatrix} \cos\theta_1 & -\sin\theta_1 & 0 \\ \sin\theta_1 & \cos\theta_1 & 0 \\ 0 & 0 & 1 \end{bmatrix} \begin{bmatrix} 1 & 0 & 0 \\ 0 & \cos\theta_2 & -\sin\theta_2 \\ 0 & \sin\theta_2 & \cos\theta_2 \end{bmatrix} \begin{Bmatrix} Ju \\ Jv \\ Jw \end{Bmatrix} \quad (2)$$

where Jx, Jy, Jz, Ju, Jv and Jw are the components of the current density $\vec{J}$.

The conductivity of the anisotropic conductor is a tensor, of which the off-diagonal elements are all zero[5]. Ju, Jv and Jw can be written using each component Eu, Ev and Ew of electric field strength $\vec{E}$ and $\sigma_\perp$ and $\sigma_{//}$ as follows:

$$\begin{Bmatrix} Ju \\ Jv \\ Jw \end{Bmatrix} = \begin{bmatrix} \sigma_\perp & 0 & 0 \\ 0 & \sigma_\perp & 0 \\ 0 & 0 & \sigma_{//} \end{bmatrix} \begin{Bmatrix} Eu \\ Ev \\ Ew \end{Bmatrix} \quad (3)$$

There exists the same relationship as Eq.(2) between Ex, Ey and Ez (x-, y- and z-components of $\vec{E}$) and Eu, Ev and Ew. By using this relationship and Eqs.(2) and (3), the relationship between Jx, Jy and Jz and Ex, Ey and Ez can be obtained as follows:

$$\begin{Bmatrix} Jx \\ Jy \\ Jz \end{Bmatrix} = [K(\theta_1)]\ [K(\theta_2)] \begin{bmatrix} \sigma_\perp & 0 & 0 \\ 0 & \sigma_\perp & 0 \\ 0 & 0 & \sigma_{//} \end{bmatrix} \times [K(\theta_2)]^{-1}\ [K(\theta_1)]^{-1} \begin{Bmatrix} Ex \\ Ey \\ Ez \end{Bmatrix} = \begin{bmatrix} \sigma_a & \sigma_b & \sigma_c \\ \sigma_b & \sigma_d & \sigma_e \\ \sigma_c & \sigma_e & \sigma_f \end{bmatrix} \begin{Bmatrix} Ex \\ Ey \\ Ez \end{Bmatrix} \quad (4)$$

where $[K(\theta_1)]$ and $[K(\theta_2)]$ correspond to the first and second matrices Eq.(2) respectively.

(b)Cable

In the case of the cable shown in Fig.3, the strand is further twisted by the angle θ_4. This is the angle between the strand and the z-axis as shown in Fig.3. Similarly, the following relationship between Jx, Jy and Jz and Ju, Jv and Jw can be obtained:

$$\begin{Bmatrix} Jx \\ Jy \\ Jz \end{Bmatrix} = [K(\theta_3)]\ [K(\theta_4)]\ [K(\theta_3)]^{-1} \times [K(\theta_1)]\ [K(\theta_2)] \begin{Bmatrix} Ju \\ Jv \\ Jw \end{Bmatrix} \quad (5)$$

where θ_3 is the angle between the e_x and e_u vectors as shown in Fig.3. $[K(\theta_3)]$ and $[K(\theta_4)]$ are the matrices of which the angles θ_1 and θ_2 in $[K(\theta_1)]$ and $[K(\theta_2)]$ are replaced by θ_3 and θ_4 respectively. The $[K(\theta_3)]^{-1}$ matrix is multiplied in Eq.(5) in order to reset the center line of the strand in the x-z plane.

The relationship between $\vec{J}$ and $\vec{E}$ in the case of the cable can be obtained in the same way as Eq.(4).

2.2 Finite Element Formulation

Galerkin's equation for the A-ϕ method can be written as follows[6]:

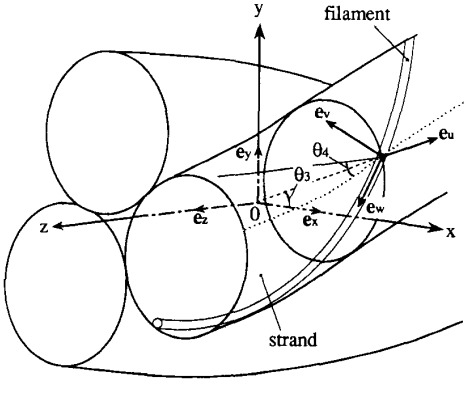

Fig.3 Cable.

$$G_i = -\iiint \mathrm{grad}N_i \times \nu\, \mathrm{rot}A\, dv + \iiint N_i \sigma \left(\frac{\partial A}{\partial t} + \mathrm{grad}\phi\right) dv \quad (6)$$

$$G_{di} = \iiint \mathrm{grad}N_i \cdot \sigma \left(\frac{\partial A}{\partial t} + \mathrm{grad}\phi\right) dv \quad (7)$$

where, A is the magnetic vector potential and ϕ is the electric scalar potential. The interpolation function N_i for the 1st-order tetrahedral element is written as follows[6]:

$$N_i = \frac{1}{6V}(a_i + b_i x + c_i y + d_i z) \quad (8)$$

where, V is the volume of an element (e). a_i, b_i, c_i and d_i are the constants determined by the coordinates of 4 nodes of the element (e). The Rayleigh-Ritz equation of the first term of Eq.(6) is the same as the usual equation[6]. The x-component G_{xi} of the second term of Eq.(6) is discretized as follows using Eqs.(4) and (8):

$$G_{xi} = \frac{j\omega V}{20} \left\{ \sigma_a \sum_{k=1}^{4}(1+\delta_{ike})\dot{A}_{xke} + \sigma_b \sum_{k=1}^{4}(1+\delta_{ike})\dot{A}_{yke} + \sigma_c \sum_{k=1}^{4}(1+\delta_{ike})\dot{A}_{zke} \right\} + \frac{1}{24}\sum_{k=1}^{4}\left\{\sigma_a b_{ke} + \sigma_b c_{ke} + \sigma_c d_{ke}\right\}\dot{\phi}_{ke} \quad (9)$$

where, δ_{ike} is Kronecker's delta and ω is the angular frequency. In Eq.(9), it is assumed that the magnetic field varies sinusoidally with time. The dot($\cdot$) shows the complex value.

Equation(7) can also be discretized in the same way as follows:

$$G_{di} = \frac{j\omega}{24}\sum_{k=1}^{4}\{ (\sigma_a b_i + \sigma_b c_i + \sigma_c d_i)\dot{A}_{xke} + (\sigma_b b_i + \sigma_d c_i + \sigma_e d_i)\dot{A}_{yke} + (\sigma_c b_i + \sigma_e c_i + \sigma_f d_i)\dot{A}_{zke}\} + \frac{1}{36V}\sum_{k=1}^{4}\{ (\sigma_a b_i + \sigma_b c_i + \sigma_c d_i) b_{ke} + (\sigma_b b_i + \sigma_d c_i + \sigma_e d_i) c_{ke} + (\sigma_c b_i + \sigma_e c_i + \sigma_f d_i) d_{ke}\}\dot{\phi}_{ke} \quad (10)$$

As the Rayleigh-Ritz equation is symmetrical as shown in Eqs.(9) and (10), the ICCG method can be applied.

3. CONDUCTIVITY OF SUPERCONDUCTOR TO BE USED IN NUMERICAL ANALYSIS

The infinite conductivity $\sigma_{//}$ of the superconductor cannot be treated in the numerical calculation. We should to determine a suitable value for the conductivity $\sigma_{//}$ in Eq.(3) for the numerical calculation.

The effects of the conductivity $\sigma_{//}$ on the coupling loss in a strand shown in Fig.4, and the number of iterations of the ICCG method are investigated. The conductivity σ_m of matrix (CuNi) and λ are assumed to be 7×10^6S/m and 0.6 respectively. Then, from Eq.(1), $\sigma_\perp$ is 2.8×10^7S/m. The relative permeability μ_r is assumed to be 0.5. The twist pitch ls of the strand is 1mm. The convergence criterion of the ICCG method is chosen as 10^{-6}. Figure 5 shows the effects of the conductivity $\sigma_{//}$ on the coupling loss and the number of iterations of the ICCG method. α is the exponent of the amplitude of $\sigma_{//}$ ($\sigma_{//}=2.8\times10^{\alpha}$ S/m). The

coupling loss increases with the conductivity $\sigma_{//}$, and it approaches a constant value when $12 \leq \alpha \leq 14$. When $\alpha > 13$, the number of iterations of the ICCG method is decreased, and unreasonable results are obtained. This may be due to the round-off error. As a result, the conductivity $\sigma_{//}$ is chosen as 2.8×10^{12}S/m ($\alpha = 12$).

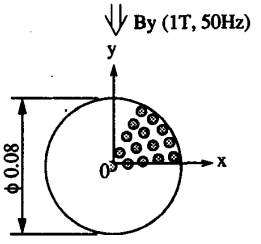

Fig.4 Model of strand.

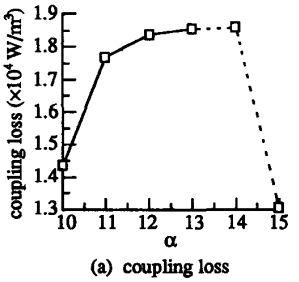

(a) coupling loss

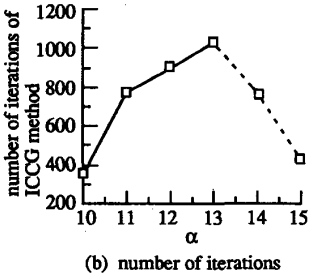

(b) number of iterations

Fig.5 Effects of $\sigma_{//}$ ($= 2.8 \times 10^{\alpha}$ S/m).

4. ANALYSIS OF COUPLING LOSSES

4.1 Comparison between Calculated and Theoretical Values of Coupling Loss in a Strand

The coupling loss in a strand shown in Fig.4 is calculated. The relative permeability μ_r is assumed to be 1.0 in order to compare the theoretical value[7]. Other constants such as $\sigma_{//}$ and $\sigma_{\perp}$ are the same as in Section 3. The calculated value ($=3.67 \times 10^4$W/m^3) is nearly equal to the theoretical value ($=3.5 \times 10^4$W/m^3). This suggests that the method proposed here may be adequate.

4.2 Coupling Losses in Stabilized Cables

3-D coupling currents in superconducting cables are analyzed. Figure 6 shows the cables stabilized with normal metal strands[8]. The 3-strand cable in Fig.6(a) is composed of 2 superconducting strands and 1 normal metal strand. The 7-strand cable in Fig.6(b) is composed of 3 superconducting strands and 4 normal metal strands. The outer diameter of the strand is all 0.1mm. The twist pitch Ls of the strand is 1mm. The twist pitch Lc of the 3-strand cable is 1.8mm, and Lc of the 7-strand cable is 3mm. The relative permeability μ_r is assumed to be 0.5. The normal metal strand is made of copper, and its conductivity is 5×10^9S/m (at 4.2°K). The matrix and sheath are both made of CuNi, and the conductivity of them are both 7×10^6S/m. The ratio λ is 0.6. The conductivity $\sigma_{//}$ parallel to the filament is chosen as 2.8×10^{12}S/m corresponding to the value found in Section 3. The conductivity $\sigma_{\perp}$ perpendicular to the filament is 2.8×10^7S/m. The contact resistances between strands are ignored. The uniform ac field (maximum flux density: 1T, frequency: 50Hz) is applied in the y-direction.

As the flux and coupling current distributions in the cable are periodic, the length of the analyzed region should be equal to Lc for the 3-strand cable and Lc/3 for the 7-strand cable. Then the lengths of the analyzed regions are 1.8mm for the 3-strand cable and 1.0mm for the 7-strand cable respectively. Figure 7 shows the mesh of the conductor region for the 3-strand cable. First-order tetrahedral elements were used, and the number of elements is equal to 12636.

Figure 8 shows the boundary conditions. The following periodic boundary conditions[9] are imposed on the boundaries at z=0 and 1.8mm respectively:

$$\mathbf{A}_p = \mathbf{A}_q, \quad \phi_p = \phi_q \tag{11}$$

where, p and q are the corresponding points on the periodic boundaries as shown in Fig.8. Ap, Aq and ϕp, ϕq are the magnetic vector potentials and the magnetic scalar potentials at the points p and q respectively. In order to apply the uniform ac field (1T) in the y-direction, the following values are given

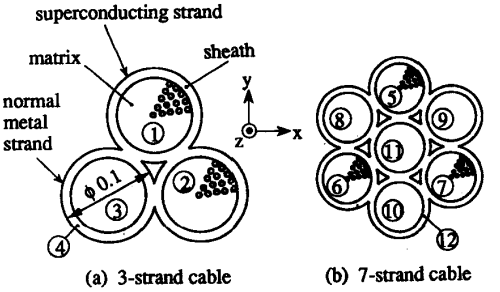

(a) 3-strand cable (b) 7-strand cable

Fig.6 Stabilized cables.

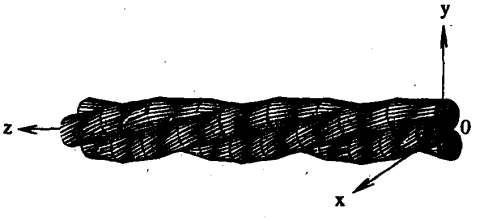

Fig.7 Mesh of 3-strand cable.

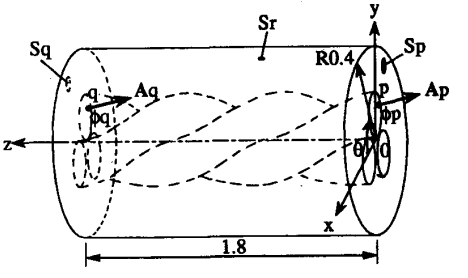

Fig.8 Boundary conditions.

for the vector and scalar potentials on the boundary Sr(r=0.4, 0<z<1.8).

$$A_x = A_y = 0, \quad A_z = 0.0004 \cos\theta, \quad \phi = 0 \qquad (12)$$

where, θ is the angle from from the x-axis.

Figure 9 shows the distributions of coupling current obtained by separating the coupling current from the total induced current at $\omega t = -90°$. Zero time is taken to be the instant when the flux density is the maximum. The length of the arrow of coupling current in the normal metal is reduced to 1/20 of the calculated value, because the amplitude of the coupling current is very large. Table I shows the comparison of coupling loss at each part per unit volume. The table denotes that the loss in the normal metal strand is about 10 times larger than that of the superconducting strand. The loss in the sheath is especially increased in the case of the 7-strand cable.

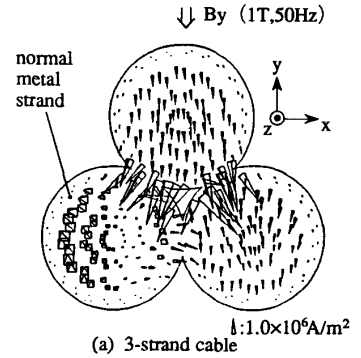

(a) 3-strand cable

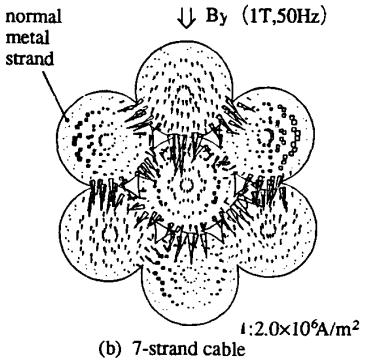

(b) 7-strand cable

Fig.9 Distributions of coupling current.

Table 1 Coupling loss in each part

(a) 3-strand cable

part	coupling loss ($\times 10^5$ W/m^3)
superconducting strand (①, ②)	0.09
normal metal strand (③)	1.04
sheath (④)	0.85

(b) 7-strand cable

part	coupling loss ($\times 10^5$ W/m^3)
superconducting strand (⑤, ⑥, ⑦)	0.14
normal metal strand (⑧, ⑨, ⑩)	1.82
normal metal strand (⑪)	1.04
sheath (⑫)	5.09

5. CONCLUSIONS

It is shown that the 3-D coupling current in a multifilamentary superconducting cable can be analyzed by treating it as a macroscopic one having anisotropic conductivity. The optimal design of an ac superconducting cable of heavy current and low loss will be possible by examining the effects of configuration of the cable, twist pitch etc., on coupling losses.

Although only the coupling loss in the absence of the transport current[2] is analyzed here, the effect of the transport current on the coupling loss should be investigated in future. The comparison of calculated and measured values of coupling losses will be reported later.

ACKNOWLEDGMENTS

The authors would like to thank Prof. T.Ogasawara of Nihon University for his useful suggestions. This work was partly supported by the Grant-in-Aid for Scientific Research (C) from the Ministry of Education, Science and Culture in Japan (No.01550224).

REFERENCES

[1] T.Ogasawara, Y.Kubota, T.Makiura, T.Akachi, T.Hisanari, Y.Oda and T.Yasukochi: "A Low Loss NbTi Multifilamentary Composite Conductor for A.C. Use", IEEE Trans. on Magnetics, MAG-19, 3, 248 (1983).

[2] W.J.Carr,Jr: "AC Loss and Macroscopic Theory of Superconductors" (1983) Gordon and Breach Science Publishers.

[3] T.Nakata, N.Takahashi, K.Fujiwara and K.Muramatsu: "Investigation of Effectiveness of Various Methods with Different Unknown Variables for 3-D Eddy Current Analysis", IEEE Trans. on Magnetics, MAG-26, 2, 442 (1990).

[4] F.Sumiyoshi, H.Kasahara, T.Kawashima and T.Tanaka: "Numerical Calculation Method of Inter-Strand Coupling Current Losses in Superconducting Conductors", Cryogenics, 29, 741 (1989).

[5] N.Takahashi, T.Nakata, Y.Fujii, S.Ikeuchi, K.Muramatsu, M.Kitagawa and J.Takehara: "Macroscopic Conductivity of Multifilamentary Superconducting Wire", Papers of Combined Convention of Chugoku Branch of IEE of Japan and Related Institutes, No.020508 (1990).

[6] T.Nakata, N.Takahashi, K.Fujiwara and M.Miura: "Finite Element Analysis of Nonlinear 3-D Magnetic Fields with Eddy Currents Using Magnetic Vector Potentials", Papers of Technical Meeting on Rotating Machinery and Static Apparatus, RM-86-39, SA-86-32 (1986).

[7] M.N.Wilson: "Superconducting Magnets" (1983) Clarendon Press.

[8] K.Funaki, O.Ichimaru, M.Iwakuma, F.Sumiyoshi, K.Miyahara and K.Yamafuji: "Increase in Coupling-Current Losses of Superconducting Cables Due to First-Stage Cabling II. Loss-Minimized Structure of Stabilized Sub-Cable", Cryogenic Engineering, 23, 1, 36 (1988).

[9] T.Nakata, N.Takahashi, K.Fujiwara and A.Ahagon: "Periodic Boundary Condition for 3-D Magnetic Field Analysis and Its Applications to Electrical Machines", IEEE Trans. on Magnetics, MAG-24, 6, 2694 (1988).